Supplementary Information (SI) for EES Batteries.

Understanding energy-power trade-off in the structure of Li-Ion battery cathodes by localized XRD: Supplementary Information

Andrew R.T. Morrison[1,2,*], Will J. Dawson[1,2,3], Hamish T. Reid[1,3], Juntao Li[2,9], Isabella Mombrini[1,4], R. S. Young[1,2], Alice V. Llewellyn[1,2], Gargi Giri[1,2,9], Partha P. Paul[4,5], Adam M. Boyce[6], Rhodri Jervis[1,2,3], Thomas S. Miller[1,2,3], James B. Robinson[1,2,3], Emma Kendrick[2,7], Philip J. Withers[5], Marco di Michiel[4], Dan J.L. Brett[8], Paul R. Shearing[2,9,*]

1:Electrochemical Innovation Lab, University College London, London, WC1E 7JE, UK
2:The Faraday Institution, Didcot, OX11 0RA, UK
3: Advanced Propulsion Lab, UCL East, University College London, London E20 2AE, UK
4: ESRF – The European Synchrotron, 71 Av. des Martyrs, 38000 Grenoble, France
5: Henry Royce Institute, Dept of Materials, University of Manchester, Manchester M1 3BB, UK
6:School of Mechanical and Materials Engineering, University College Dublin, Dublin D04V1W8, Ireland
7:School of Metallurgy and Materials, University of Birmingham, Edgbaston, Birmingham, BT15 2TT, UK
8:Prosemino Ltd, Paper Yard, Quebec Way, London SE16 7LG
9: The ZERO Institute University of Oxford., Holywell House, Osney Mead, Oxford, OX2 0ES
**: Corresponding Authors*

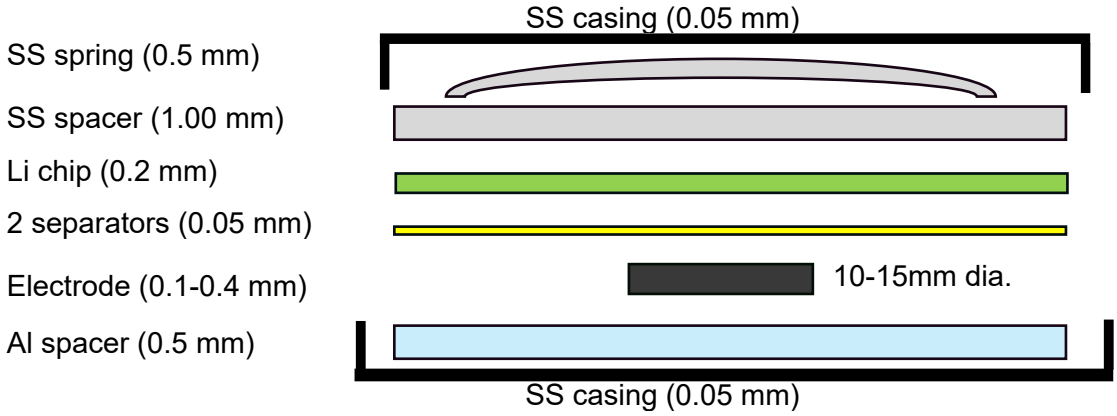

Figure S1: 2032 coin cell configuration used in this study. The major differences to the standard configuration are; the Al spacer instead of steel (to reduce x-ray attenuation for escaping x-rays), the double separator (for more reliable operation), and the smaller cathode to optimize beam transmission.

Table S1: The properties of a thinner electrode, as in Table 1 in the main text. This electrode was also used for operando measurements and it has similar results to the electrode discussed in the main text as seen in section S2.

Electrode Radius	2.5mm
Crack Intensity Factor[3]	2.14%
NMC Loading	21 mg/cm^2
Wet Coat thickness	600 µm
Dry Thickness	145 µm
Crack of Interest Length	700 µm
Crack of Interest Width	40 µm
Capacity @Formation	0.68 mAh

Specific Capacity @ Formation	165 mAh/g
Aerial Capacity	3.46 mAh/cm^2
Measurement Depths	U=30, M=70, B=110 µm

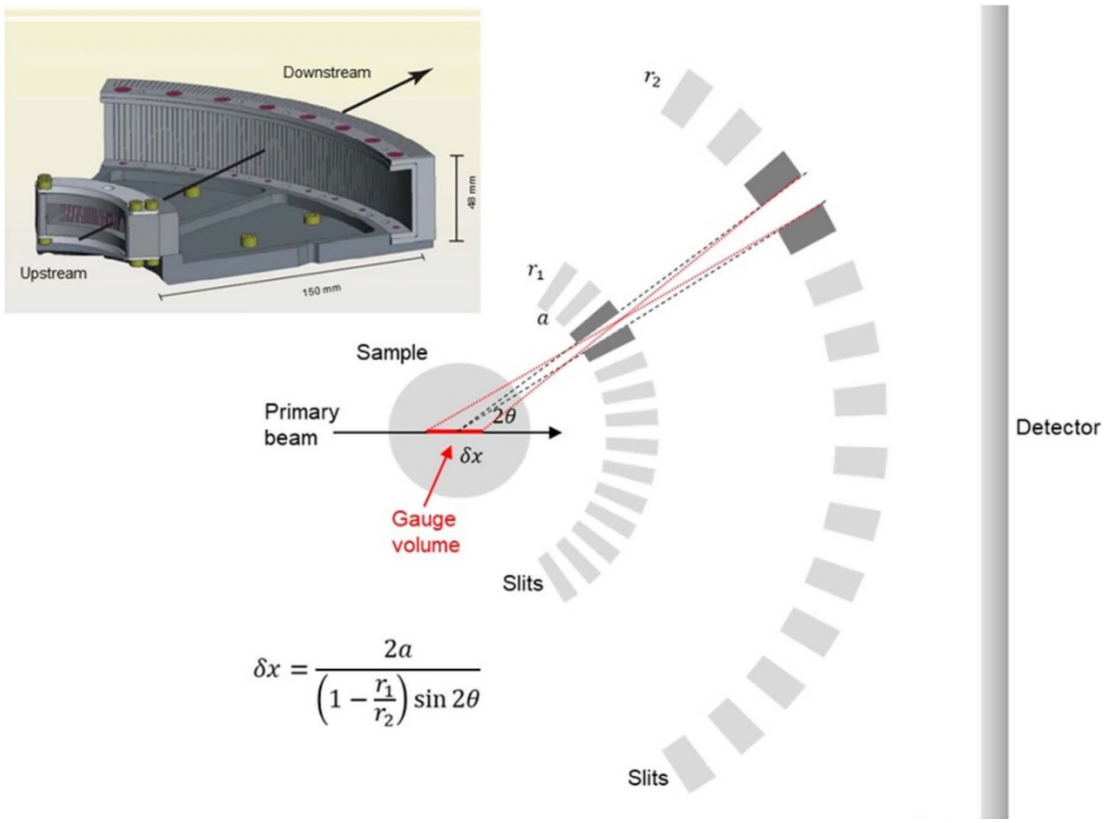

Figure S2: 3D rendering and plan view of the Multi-channel collimator configuration (adapted from literature[1, 2]). The length of the gauge volume is given by equation 1 in the main text, the dimensions perpendicular to the beam are the dimensions the beam (10 x 10 µm). The schematic shows how the MCC is able to supress all diffracted rays except those coming from the gauge volume.

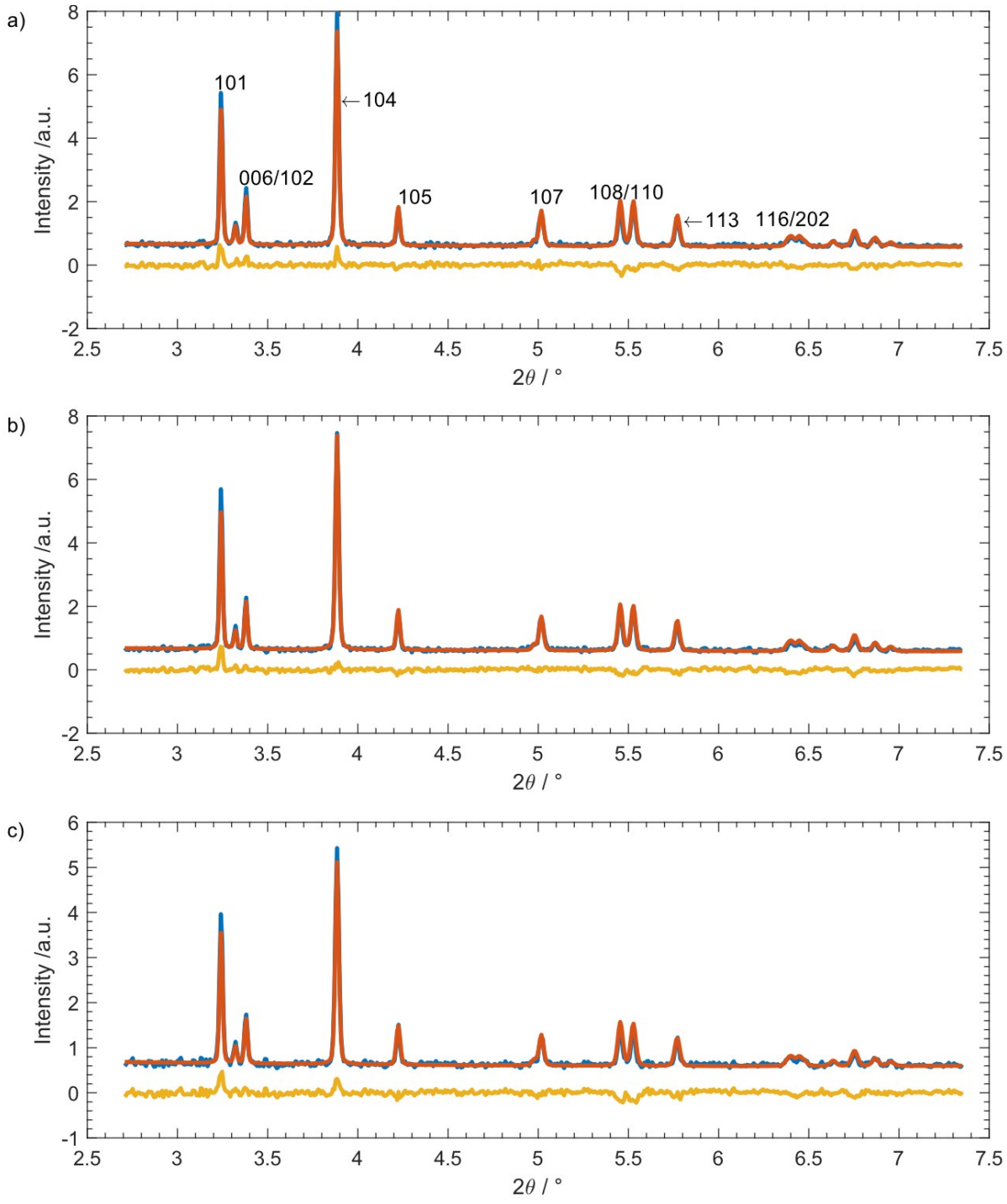

Figure S3: Example intensity vs. 2θ from the first set of scans of the 0.8C cycle for the bottom level a) in the bulk, b) in the middle), c) near crack locations in the electrode. Blue is data, orange is fit, and yellow is the residual. Note that the higher 2θ peaks in the near crack pattern are less intense and sometimes not discernable from the background. However, since d-spacing is the key element in our analysis, even the lower 2θ reflections will give sufficient information, especially when averaged together.

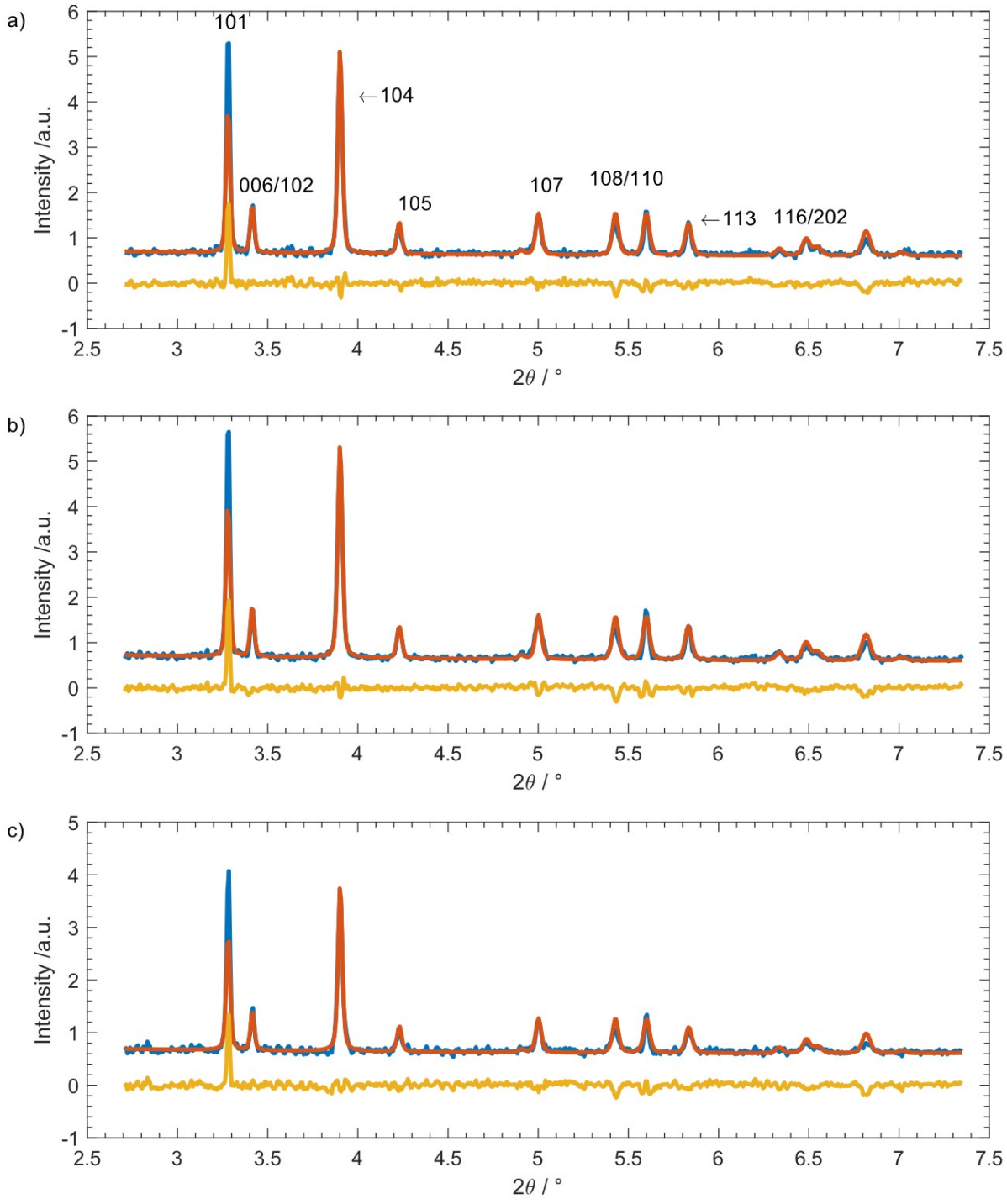

Figure S4 Example intensity vs. 2θ from the set of scans at top of charge of the 0.8C cycle for the bottom level a) in the bulk, b) in the middle), c) near crack locations in the electrode. Blue is data, orange is fit, and yellow is the residual. Note how the 101 reflection peak height becomes systematically underestimated. This is possibly due to cation mixing, but because we are unable to use the 003 peak in this analysis to confirm we can be less certain. In any case, it does not effect fitting of peak position, so the calculation of state of lithiation is unaffected.

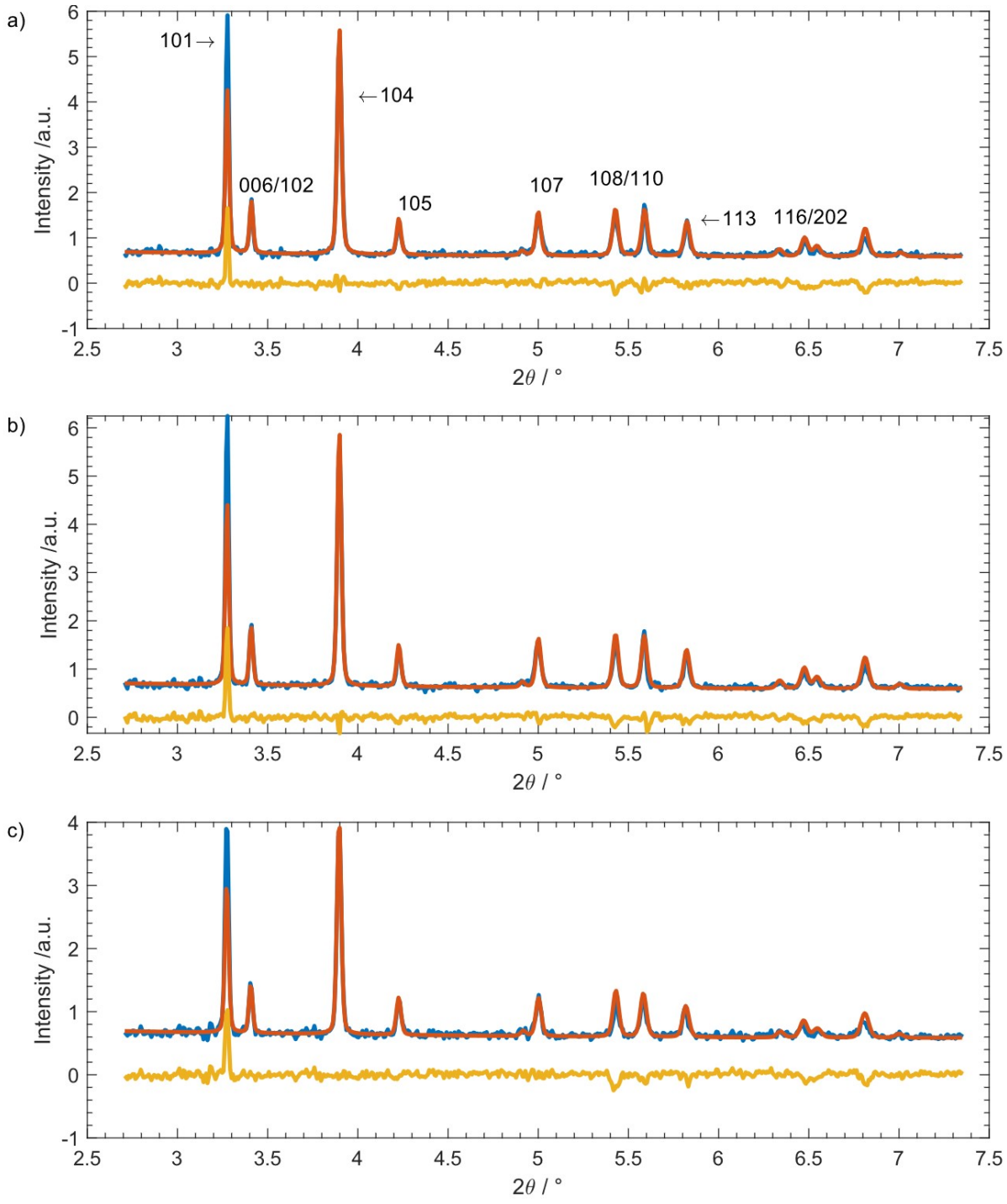

Figure S5 Example intensity vs. 2θ from the set of scans at the end of discharge of the 0.8C cycle for the bottom level a) in the bulk, b) in the middle), c) near crack locations in the electrode. Blue is data, orange is fit, and yellow is the residual. Note how the 101 peak height is still systematically underestimated, but less than at top of charge, again difficult to interpret without access to the 003 peak, but it still does not effect peak position fit.

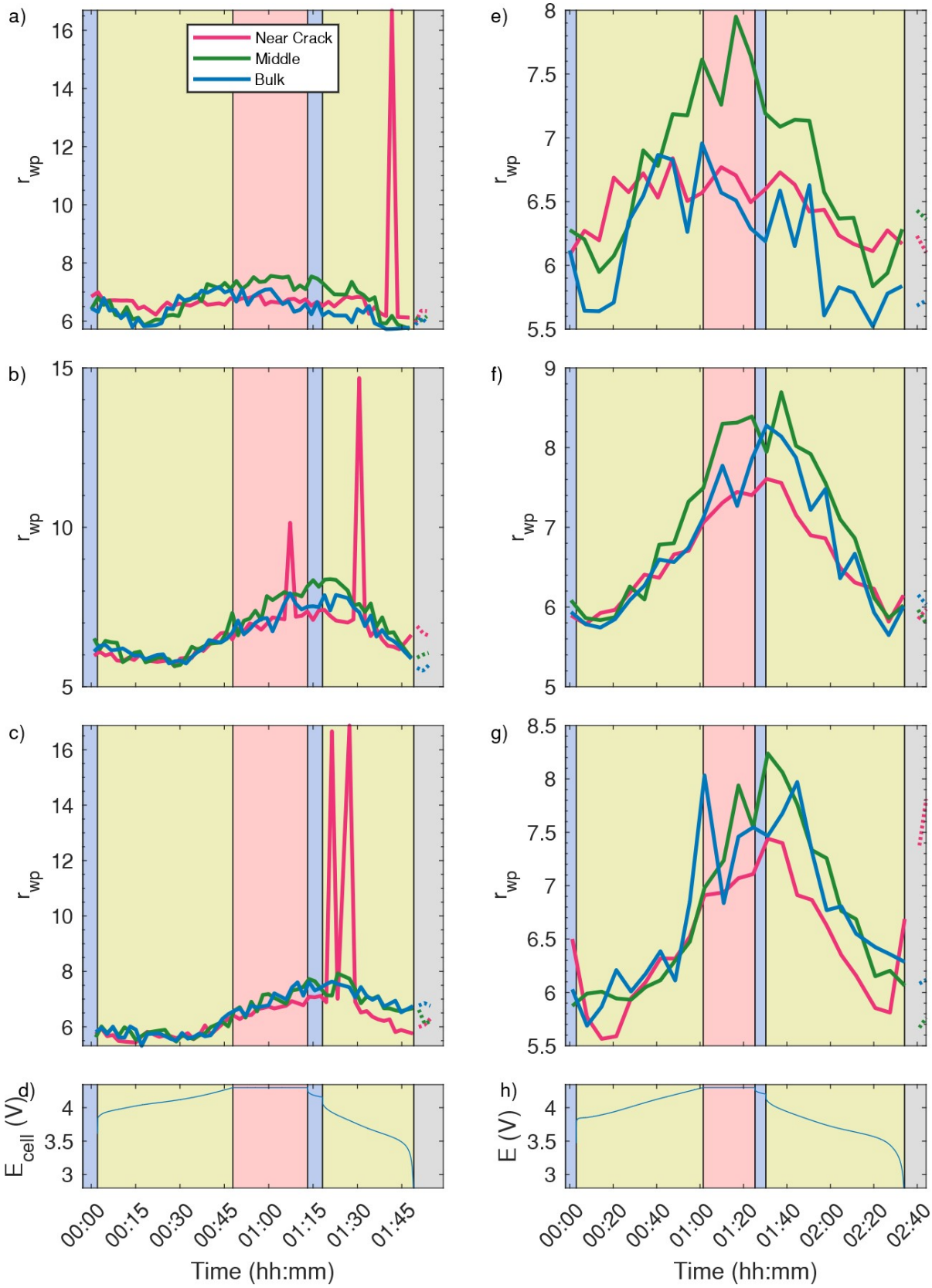

Figure S6: A goodness of fit parameter for two of the cycles of the thick electrodes studied in the main text. The traces show average values from the same sets of points for pink ("near crack"), green ("middle"), and blue ("bulk"), similar to figure 5 in the main text. The background colours indicate the electrochemical state. Blue: open circuit, yellow: constant current charge or discharge, red: constant voltage charge, and grey constant current discharge at half the nominal rate. Lines become dashed after the nominal cycle ends. While the 0.8 C cycle has a couple of large spikes, even these values show a good fit to the data

(see Figure S7 to see plots of individual XRD patterns corresponding to the outlier points). There is also a dependence on charge condition, but again, all values show a good fit.

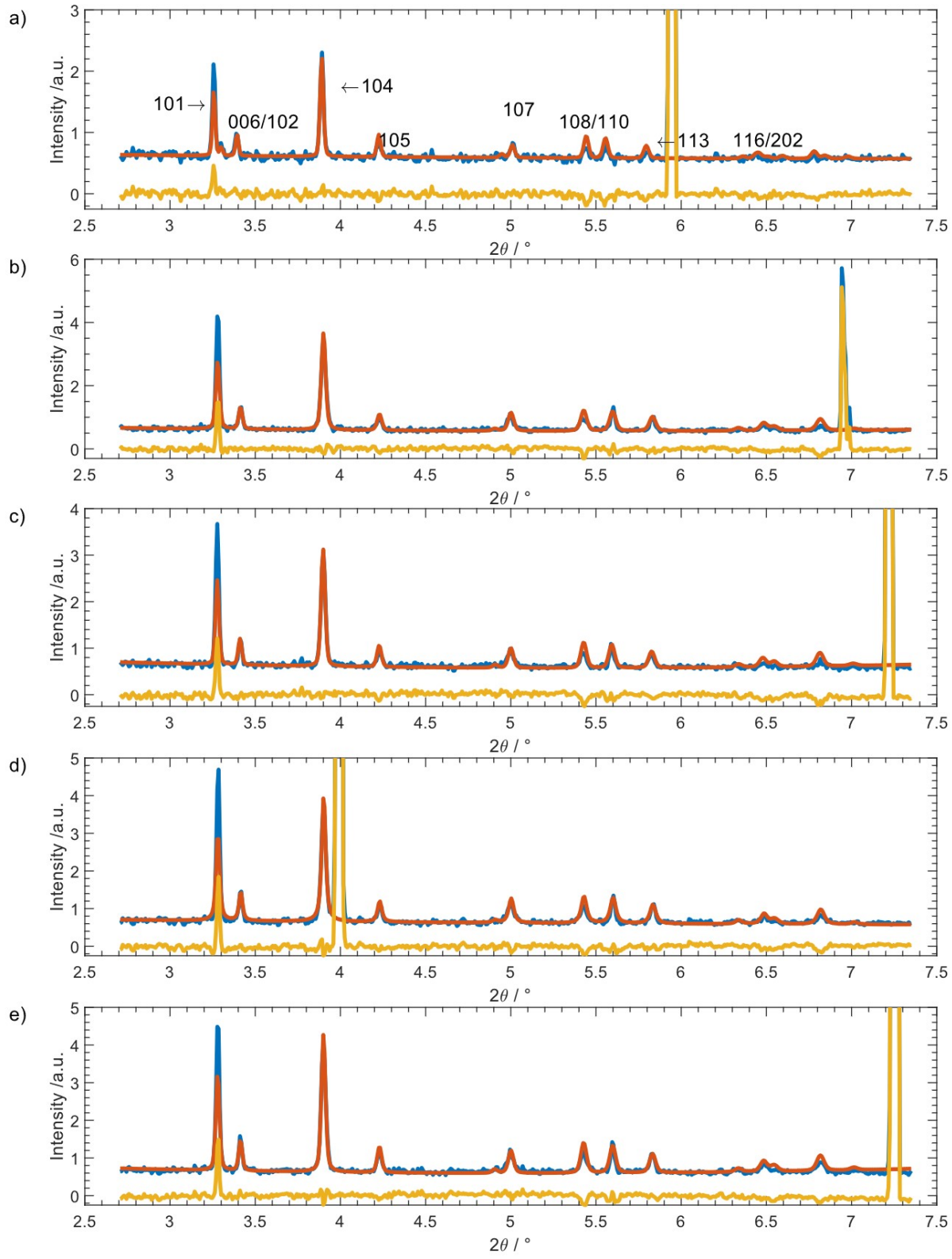

Figure S7: Intensity vs 2θ for the 5 outlier points visible Figure S6 In the order they appear in that figure from left to right and top to bottom (e.g. a) in this figure is the outlier in figure S6 a), and e) here is the right most outlier in Figure S6 c)). As can be seen, the higher r_{wp} seen in Figure S6 is due to anomalous spikes in intensity, unrelated to the NMC pattern. Despite these anomalous peaks, the refinement remains very accurate with respect to the peak positions, and this is the key feature for the purposes of this work because that is what is related to the SoL.

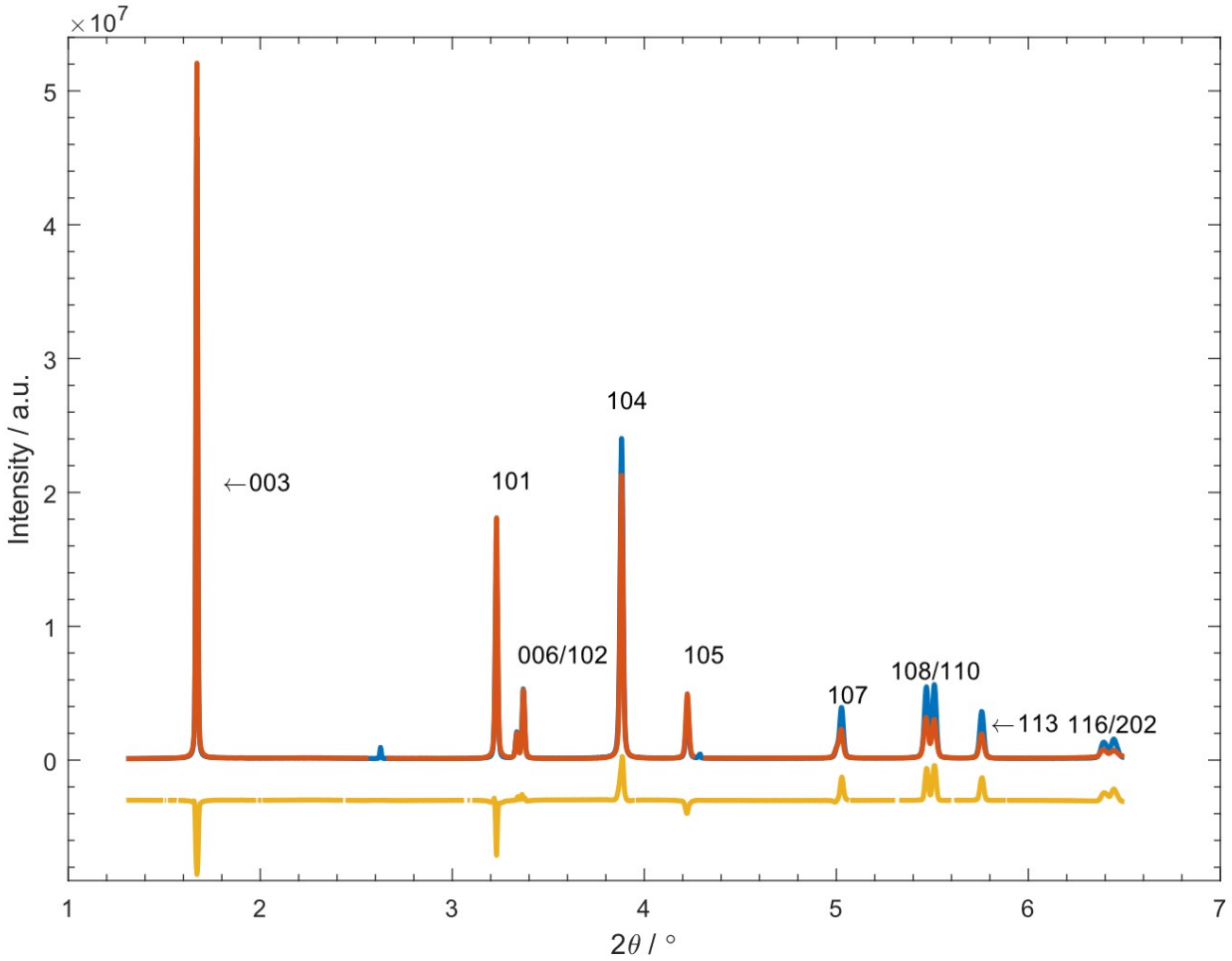

Figure S8: XRD pattern and refinement for pristine NMC622 collected at ID15A at ESRF through an XRD-computed tomography approach. It is from the average from the centre 1mm of a cast electrode of the same NMC622 as used in the operando research in this study. The interpolated state of lithiation (calculated in the same way as for the operando data, see section S1) for the pristine material is 0.96 – higher than observed in operando in this study, but some decrease is expected after the initial formation cycles.

S1: State of Lithiation Calculation and Uncertainty Propagation

State of lithiation is estimated from the unit cell volume and published values from the XRD refinements of NMC 622 at different lithiations states from a slowly cycled cell from de Biasi et al[4]. The refinement of the XRD patterns in this work give the unit cell dimensions, which then give the unit cell volume. The state of lithiation is calculated from the unit cell volume via linear interpolation. From the unit cell dimensions which are obtained via refinement the process is thus

$$Vol = a \cdot a \cdot c \cdot \sin(60)$$

where *a* and *c* are the unit cell dimensions and *Vol* is the volume of the unit cell. Functionally, this value is calculated within TOPAS and the uncertainty in *a* and *c* from refinement (*δa* and *δc*) is propagated to *δVol* with in the software. Then *SoL* is calculated according to a linear interpolation:

$$SoL = SoL_{REF1} + (Vol - Vol_{REF1}) * \frac{SoL_{REF2} - SoL_{REF1}}{Vol_{REF2} - Vol_{REF2}}$$

where (Vol_{REF1}, SoL_{REF1}) and (Vol_{REF2}, SoL_{REF2}) are the two pairs of volume and associated state of lithiation according to de Biasi et al[4] which are closest to the queried volume (Vol). The uncertainty is propagated to SoL according to the partial derivative method which gives

$$\delta SoL = \sqrt{\begin{aligned} &\left(\frac{SoL_{REF2} - SoL_{REF1}}{Vol_{REF2} - Vol_{REF2}}\delta Vol\right)^2 \\ &+ \left(\frac{(SoL_{REF2} - SoL_{REF1})(Vol - Vol_{REF2})}{(Vol_{REF2} - Vol_{REF2})^2}\delta Vol_{REF1}\right)^2 \\ &+ \left(\frac{(SoL_{REF2} - SoL_{REF1})(Vol_{REF1} - Vol)}{(Vol_{REF2} - Vol_{REF2})^2}\delta Vol_{REF2}\right)^2 \\ &+ \left(\left(1 - \frac{Vol - Vol_{REF1}}{SoL_{REF2} - SoL_{REF1}}\right)\delta SoL_{REF1}\right)^2 \\ &+ \left(\left(\frac{Vol - Vol_{REF1}}{SoL_{REF2} - SoL_{REF1}}\right)\delta SoL_{REF2}\right)^2 \end{aligned}}$$

where δ denotes the uncertainty in a give variable. This formula accounts for uncertainty in all parameters, both the refined values from our measurements and the uncertainty in the values used for interpolation (which are published in the same source). Uncertainty in averaged values are calculated with the same method.

S2: MCC-XRD Refinement and Gauge Volume Length

To investigate the robustness of the XRD refinements presented several different restricted 2θ refinements were performed (where a subset of the full range of 2θ available is used). The purpose of these refinements is two-fold. First, recovering the same pattern of lithiation discussed in the main text from a smaller 2θ range shows that our refinements are robust. See Figure S9 for example results (showing just the bottom layer of the 0.5 C cycle) using different 2θ ranges for refinements of the cell described in the main text. As can be seen, the essential pattern of when separation in SoL of the different layers occurs is persevered for all ranges of 2θ.

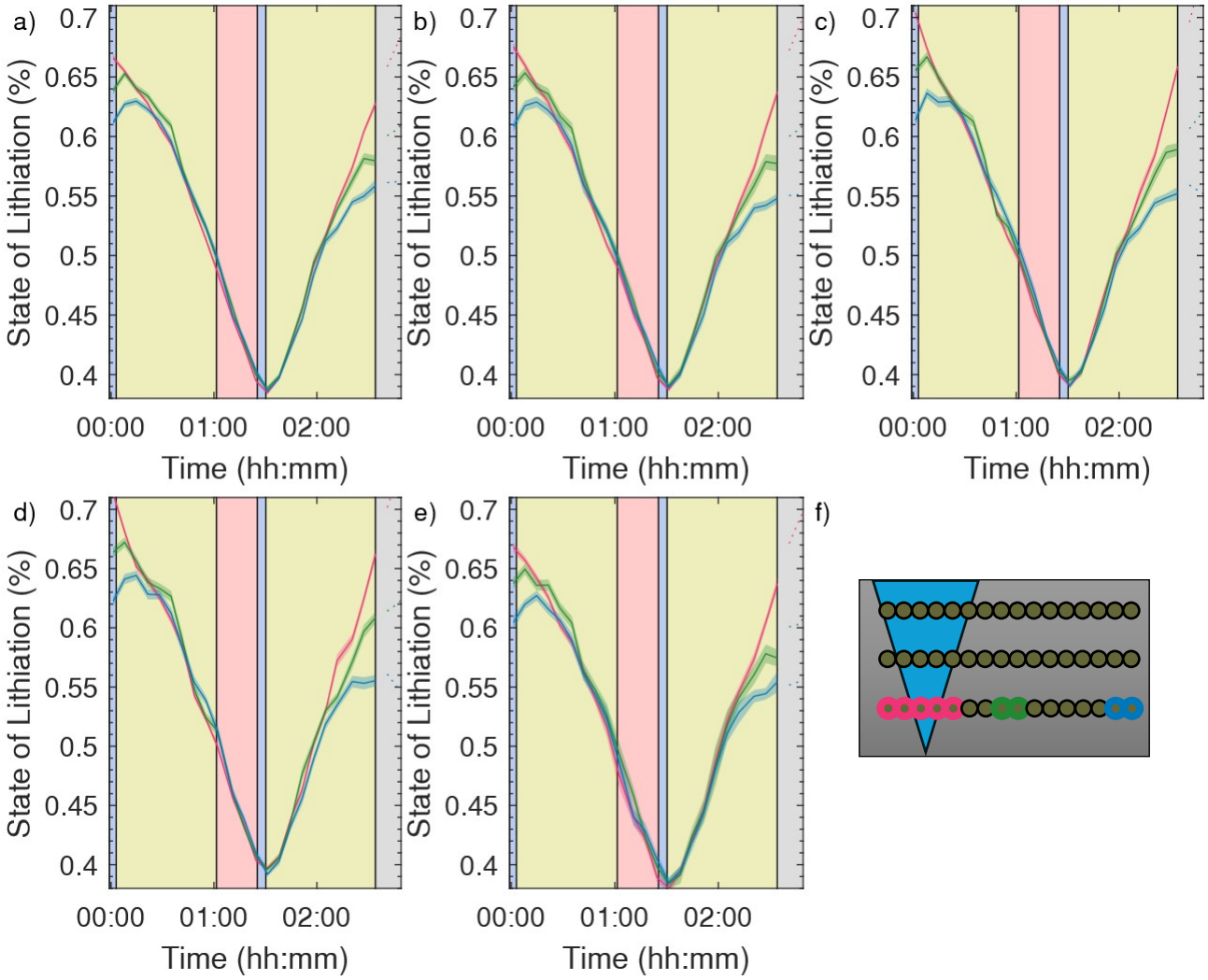

Figure S9: Several examples of SoL time evolution plots for different 2θ ranges. In each case it is the SoL for the bottom layer (with displayed points shown in the cutaway) during the 0.5C cycle of the thicker electrode. a) Is the range used in the main text 2.8–7.35° b) is 3.3–7.35° (lowest angle reflection included is 104) c) is 3.9–7.35° (lowest angle reflection included is 108) d) is 5.25–7.35° and e is just the lower angles 2.8–4.1°, (which include only the 101, 006, 102 and 104 reflections).

The low 2θ range (Figure S9 a) shows the refinement is not dependent on the low magnitude reflections found at high angles. All the important information is contained in the well-defined reflections (101, 104, 006, and 102). This makes sense, since a reflection's 2θ position is the most important feature for the purpose of this work. This is because that is what will determine the refined lattice spacing, which determines the refined unit cell volume, which determines the SoL (see section S1, above). At a minimum, the lattice spacing can be determined in the case of NMC by any two linearly independent reflections. Refining further reflections will only increase confidence, as long as the reflection positions are all consistent (i.e. as long as the model is correct). Normally, this would be guaranteed to be the

case, however in the specific case of MCC there is a small wrinkle which connects to the second reason to do refinements on constricted 2θ ranges. That wrinkle is that the length of the gauge volume depends on the 2θ (equation 1, in the main text). That means for different reflections, the crystal grains contributing to the observed reflection changes as the gauge volume length changes. This explains the small variation between the different 2θ ranges – refining different combinations of reflections represents slightly different mixing of gauge volume length. The higher 2θ ranges (Figure S9 c,d) do show a slightly larger separation of SoL, which could be consistent with a shorter gauge volume length catching less of the ends of the crack.

This effect provides an interesting lens through which to examine the second cell studied (See table Table S1 and Figure 1 b in the main text). The crack in the electrode in that cell is about half the length of the crack in the electrode discussed in the main text. That means a large overhang for the gauge volume of the 101 reflection is already expected, and indeed the results of the analysis for this electrode in the same 2θ range as the main text electrode shows different results. This can be seen in Figure S10, where the lowest angle refined goes from 2.8° (a), to 5.25° (d) with corresponding gauge volume lengths of 1.3 mm, 1.07 mm, 0.83 mm, and 0.77mm.

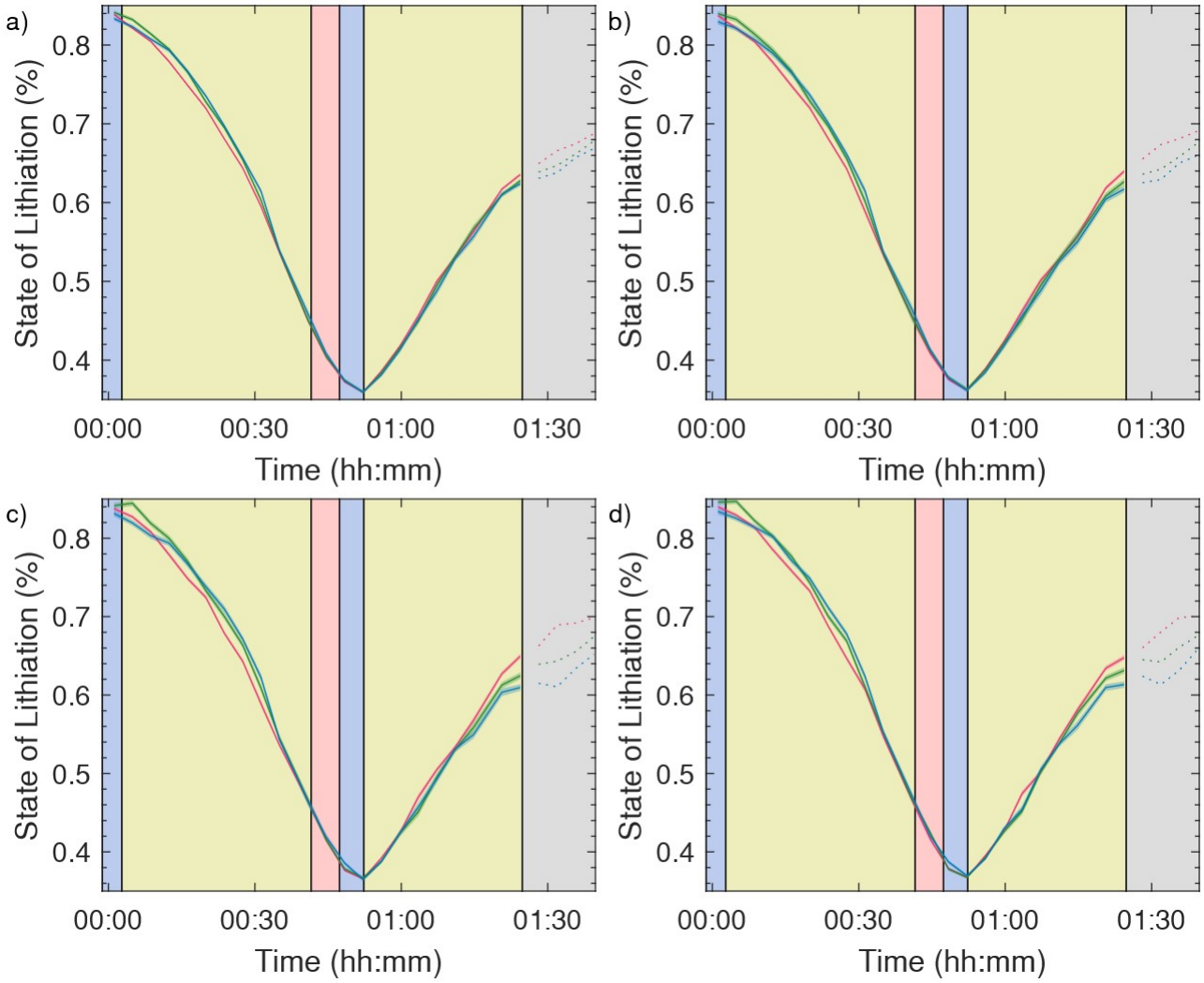

Figure S10: Time evolution of SoL for different 2θ ranges for 1.35C cycle of the thinner electrode. a) Is the range used in the main text 2.8–7.35° b) is 3.3–7.35° (lowest angle reflection 104) c) is 3.9–7.35° (lowest angle reflection 108) d) is 5.25–7.35°. This corresponds to 1.3 mm (a), 1.07 mm (b), 0.83 mm (c) and 0.77mm (d) gauge volume length.

However, if the 2θ range is restricted to include only the 107 reflection and higher angles we can recover the same phenomena observed in the main text. This is consistent with the length of the gauge volume as well (the crack is 700 μm and the gauge volume length at the 107 reflection 2θ is ~ 800 μm).

Using this restricted angle refinement we can thus compare the results more directly from the thinner electrode with the thicker electrode as a replication. In the first cycle the rate is slow enough that very even lithiation is observed (Figure S11a-d), there is no separation between the regions near the crack or far from it even at the deepest level of the electrode. The essential features of the analysis of the electrode from the main text are visible again (e.g. a separation of SoL between near the crack and the bulk), Figure S11, S12 and S13 though some of the subtlety is missing. This can be ascribed to the combination of facts 1: the gauge volume still overhangs the crack and 2: the smaller gauge volume length makes local variation in bulk electrode geometry more significant.

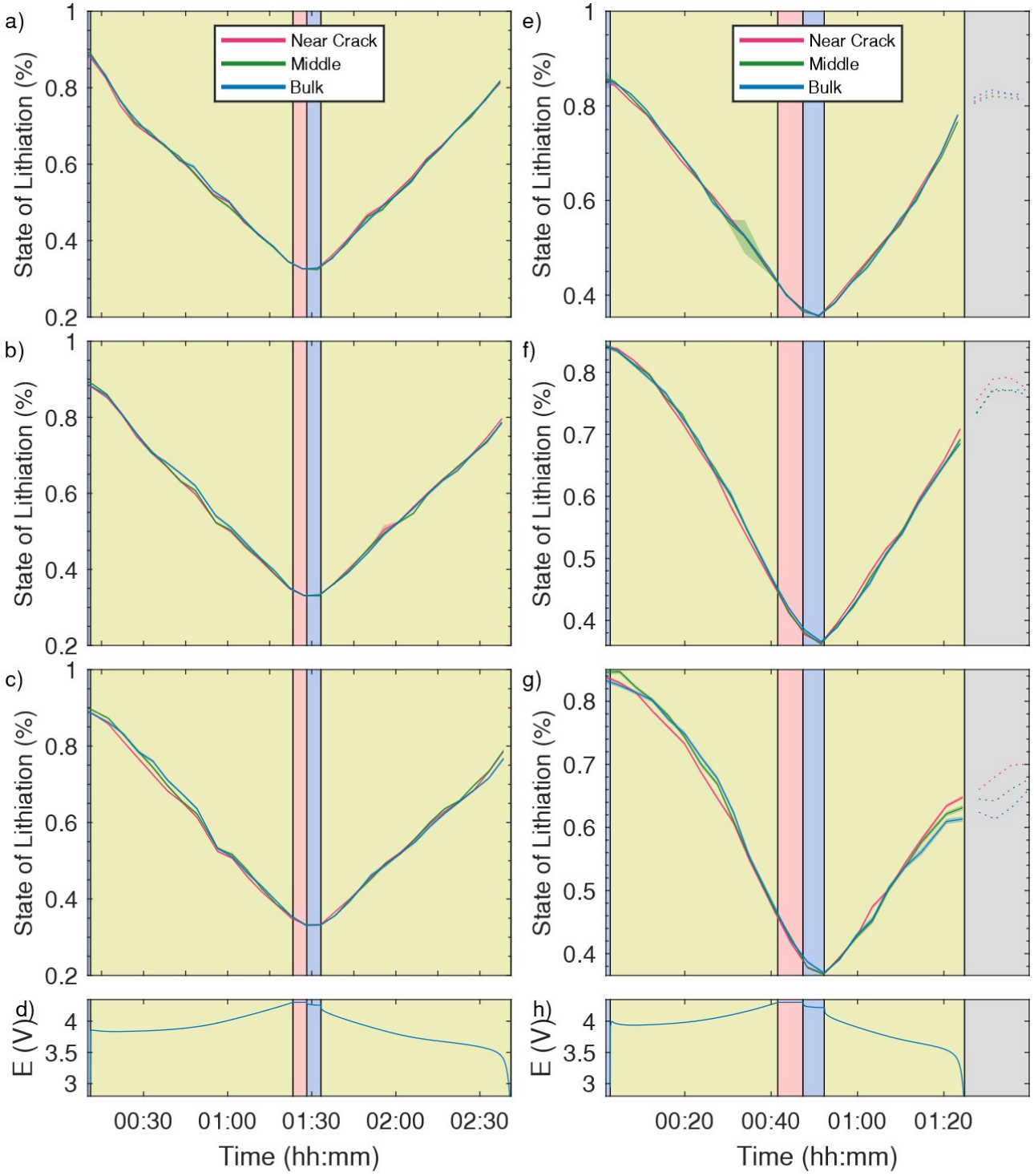

Figure S11 Time Evolution of SoL for the thin electrode in the 0.75C (a-d) and 1.15C cycles (e-h), for a refinement restricted to 5.25–7.35° for a 0.77mm gauge volume. The top most (a, e) being the top most layer, the bottom most (c,g) being the layer nearest the current collector, and (b, f) being the mid layer (d,h) is the voltage profile). Each curve is additionally surrounded by a confidence interval, which corresponds to the statistical uncertainty from refinement. Each curve is average of 2 (middle and bulk) or 5 (near crack) MCC-XRD point measurements. In all plots the background colour is synchronized to electrochemical state: Blue: Open Circuit, Yellow: constant current, pink: Constant Voltage, grey: slow CC discharge. The slow discharge in the grey is at 0.4C, which is why the SoL curves continue to separate after the end of the yellow section. The SoL curves are additionally shown in dotted during the slow discharge to distinguish them.

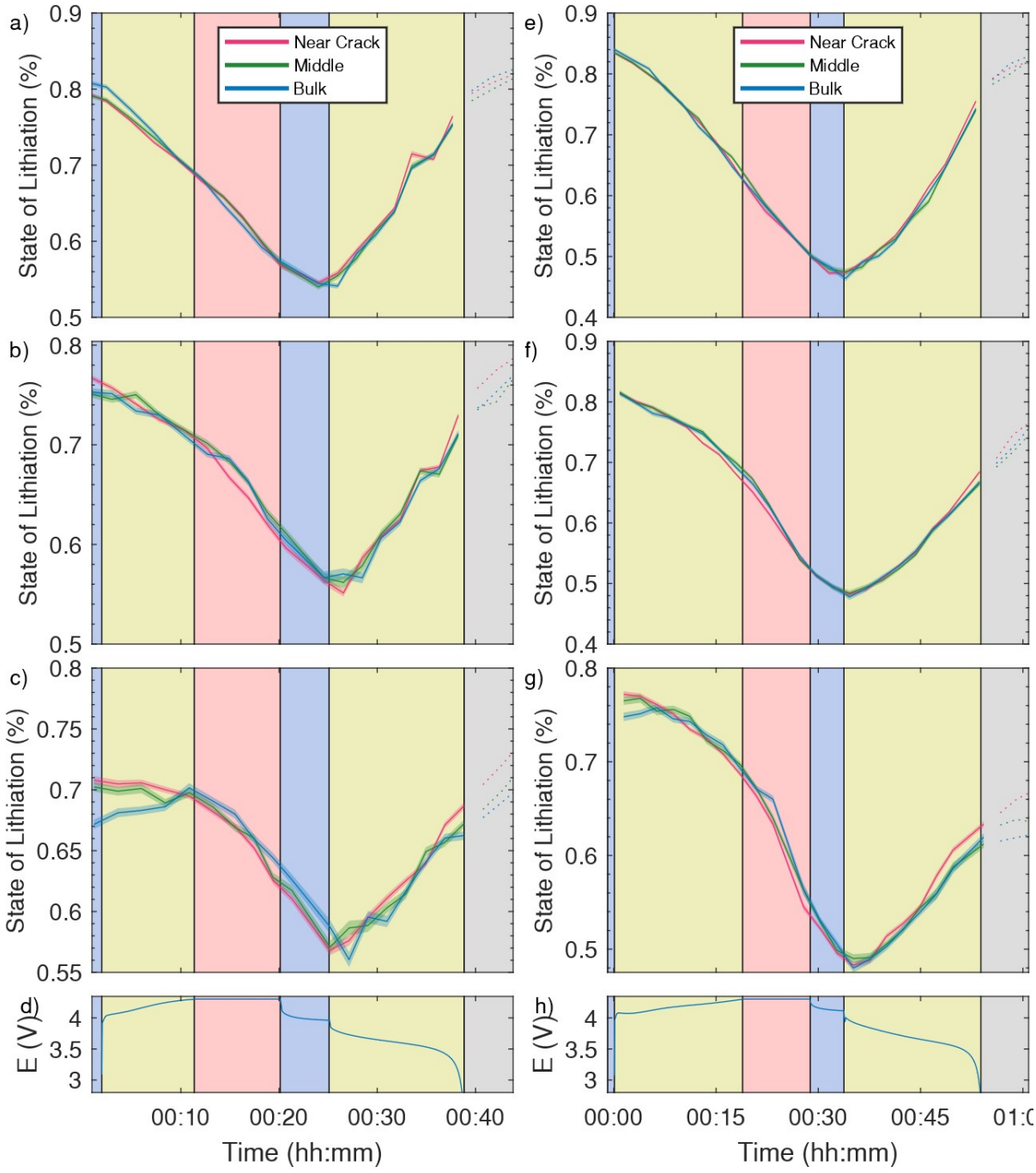

Figure S12: Time Evolution of SoL for the thin electrode in the 1.5C (a-d) and 1.35C cycles (e-h), for a refinement restricted to 5.25–7.35° for a 0.77mm gauge volume. The form of the graphs are presented in the same form as Figure S11.

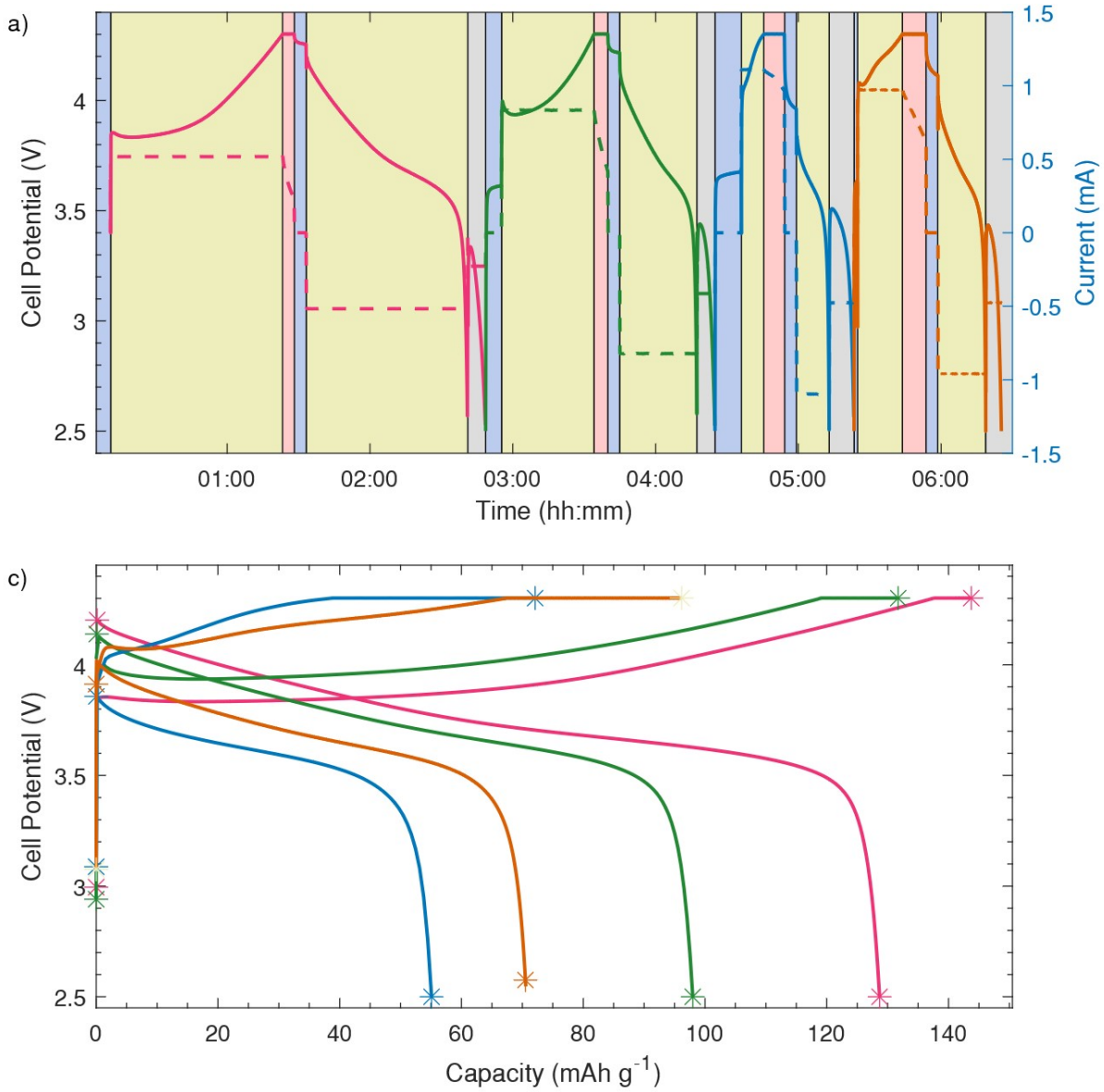

Figure S13 The thin electrode (seen in figure 1 in the main text) was cycled symmetrically at 0.75C, 1.15C, 1.5C and then 1.35 C.

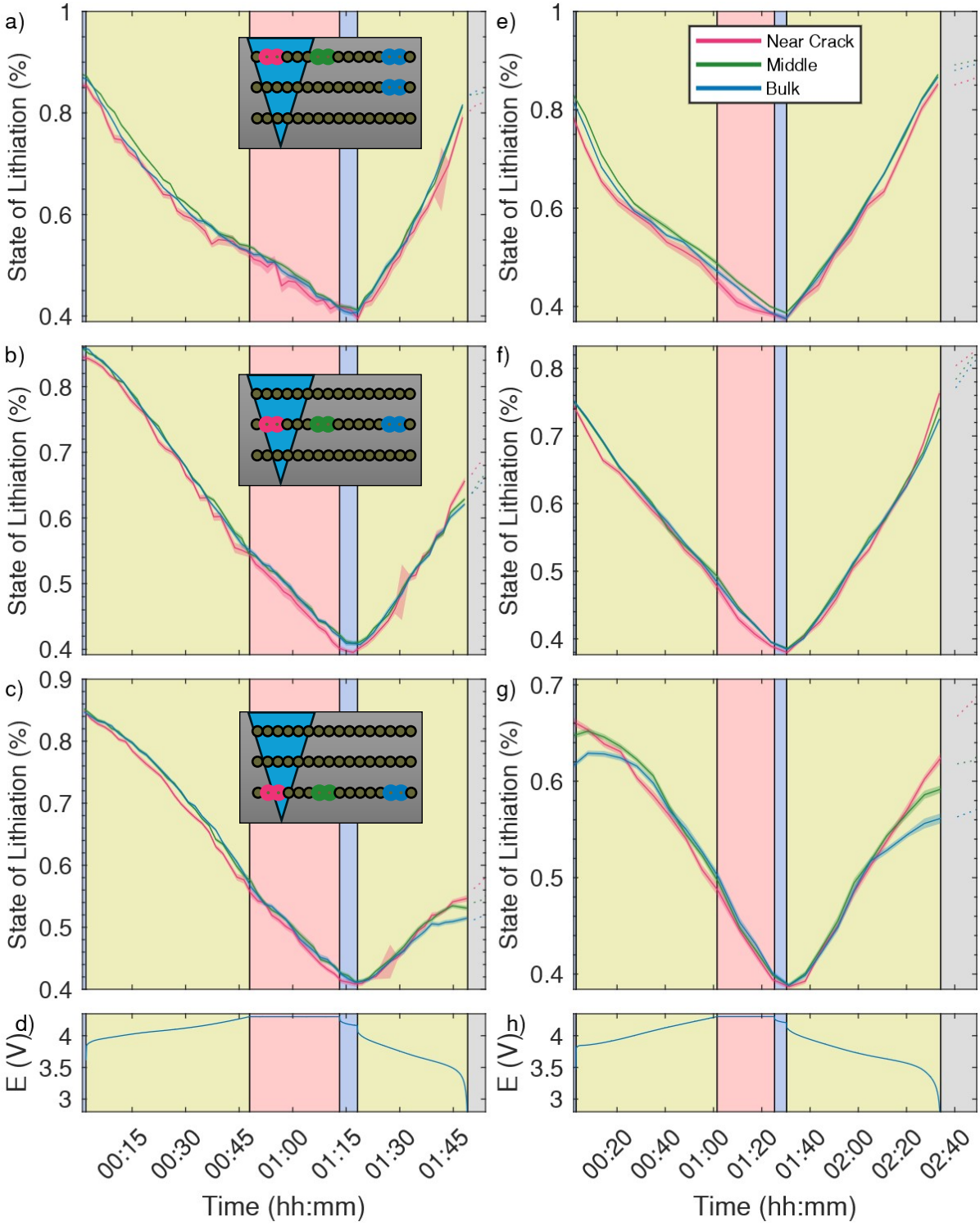

Figure S14: Time evolution of SOC for the 0.8 and 0.5 C cycles, but for different groupings of MCC points to show the effect that choice of grouping has. The "bulk" and "Middle" groupings have been shifted 1 toward the crack, and the "Near Crack" points have been restricted to only 2 points. The positions are shown in the insets which show a cross section of the measurement positions in a,b and c which also apply to the figure to the right (respectively to e, f and g). The form of the graphs are presented in the same form as Figure S11.

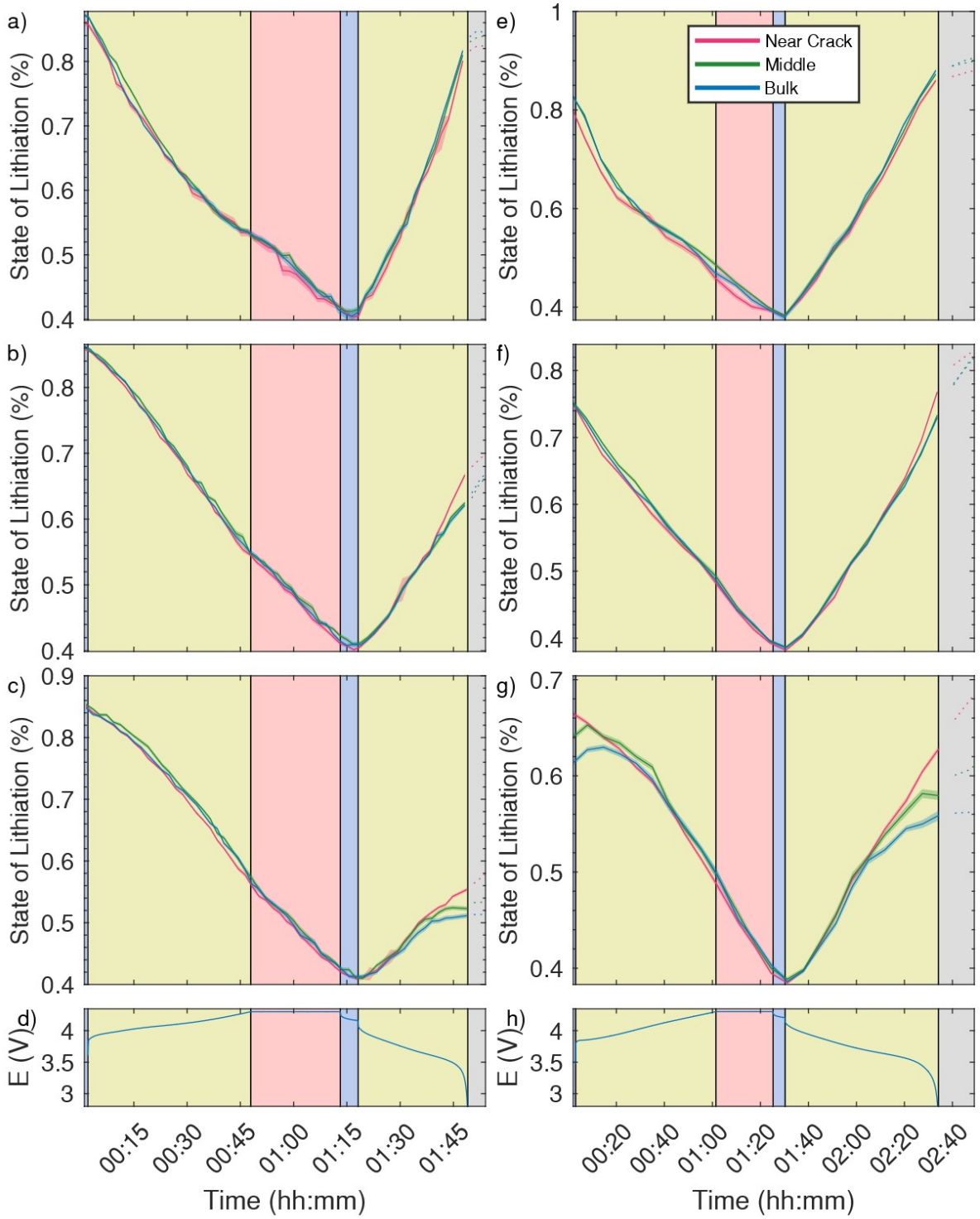

Figure S15: The SoL time evolution of the 0.8C and 0.5C cycles of the thicker electrode, as seen in Figure 4 in the main text, but each level is separated out into it's own sub figure. The 0.8C cycle plots are a-d, with the top most (a) being the top most layer, the bottom most (c) being the layer nearest the current collector, and (b) being the mid layer (d) is the voltage profile). The 0.5C cycle plots are e-h with the same organization as 0.8C: e) is the top most layer, f) the mid layer and g the layer closest to the current collector (and h the voltage profile). Each curve is additionally surrounded by a confidence interval, which corresponds to the statistical uncertainty from refinement. Each curve is average of 2 (middle and bulk) or 5 (near crack) MCC-XRD point measurements. cycle. In all plots the background colour is synchronized to electrochemical state: Blue: Open Circuit, Yellow: constant current, pink: Constant Voltage, grey: slow CC discharge. The slow discharge in the grey is at 0.4C, which is why the SoL curves continue to separate after the end of the yellow section. The SoL curves are additionally shown in dotted during the slow discharge to distinguish them.

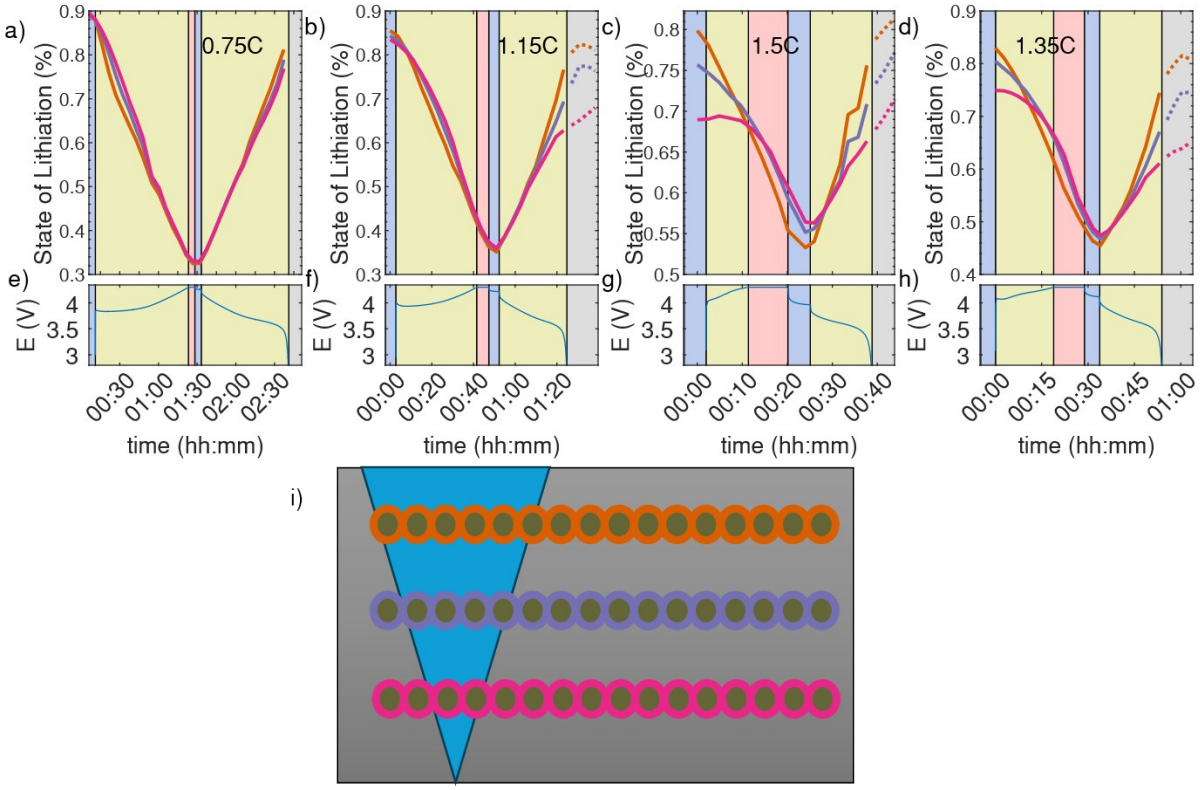

Figure S16 : Time evolution of state of lithiation of different regions of the thin electrode with the standard 2θ range (therefore standard gauge volume length) 2.8–7.35° and the cell voltage during the a),e) 0.75C and b),f) 1.15C, c),g) 1.5C and d),h) 1.35C cycle as computer from MCC-XRD measurements. In each SOL plot the orange curve is near the surface, purple in the middle of the electrode and pink is near the bottom of the current collector. Each curve is average all of the MCC-XRD point measurements at the specified level, this is schematically shown in i), with a schematic highlighting all the averaged points for each colour of curve. In all plots the background colour is synchronized to electrochemical state: Blue: Open Circuit, Yellow: constant current, pink: Constant Voltage, grey: slow CC discharge.

References

1. K. Yaoita, Y. Katayama, K. Tsuji, T. Kikegawa and O. Shimomura, *Review of Scientific Instruments*, 1997, **68**, 2106-2110.
2. T. M. M. Heenan, I. Mombrini, A. Llewellyn, S. Checchia, C. Tan, M. J. Johnson, A. Jnawali, G. Garbarino, R. Jervis, D. J. L. Brett, M. Di Michiel and P. R. Shearing, *Nature*, 2023, **617**, 507-512.
3. W. J. Dawson, A. R. T. Morrison, F. Iacoviello, A. M. Boyce, G. Giri, J. Li, T. S. Miller and P. Shearing, *Batteries & Supercaps*, 2024, **7**, e202400260.
4. L. de Biasi, A. O. Kondrakov, H. Geßwein, T. Brezesinski, P. Hartmann and J. Janek, *The Journal of Physical Chemistry C*, 2017, **121**, 26163-26171.